

Spin-lattice relaxation of dipolar order in paramagnetic-impurity-doped CaF_2 [†]

L. J. Humphries* and S. M. Day

Department of Physics, University of Arkansas, Fayetteville, Arkansas 72701

(Received 27 May 1975)

Pulse NMR techniques have been used to study the spin-lattice relaxation of dipolar order in single crystals of CaF_2 doped with either Mn^{2+} or Ce^{3+} paramagnetic ions. The spin-lattice relaxation time of dipolar order, T_1^d , has been obtained as a function of impurity concentration, temperature, and field orientation. An initial nonexponential dependence in dipolar relaxation was observed. The method of adiabatic demagnetization in the rotating frame, for creating dipolar order, was compared with the pulse method proposed by Jeneer and Broekaert, and differences in the resulting relaxation have been noted. Finally, T_1^d has been compared with the rotating-frame relaxation time T_1^r , and no correlation between the two was found.

I. INTRODUCTION

Nuclear magnetic resonance (NMR) has been a fruitful tool for studying interactions in solids. In particular, spin-lattice relaxation of nuclear spins via electron paramagnetic impurities has received considerable attention since Bloembergen¹ first proposed the relaxation mechanism in 1949. The extension of the theory of spin-lattice relaxation via impurities to the rotating frame by Lowe and Tse² added a new dimension which allowed a more definitive test of the relaxation mechanism.

Several years ago an experiment using the rare-spin detection method^{3,4} was initiated to study the magnetic environment of nuclear spins near a paramagnetic impurity. Instead of spin locking³ the bulk spins (spins far from the impurities), a method of adiabatic demagnetization in the rotating frame (ADRF) similar to that of Lurie and Slichter⁵ was used to create an ordered dipolar state. Before proceeding with the original experiment, it was necessary to study impurity-induced relaxation of dipolar order. Since there was no theory for relaxation of dipolar order by means of paramagnetic impurities, samples which were studied by Tse and Lowe⁶ in their rotating-frame relaxation experiments were used to provide some means for comparison. Their experimental results confirmed their theory and allowed them to obtain values for the correlation time τ_c of the paramagnetic-impurity spins. In our experiments, the characteristic time for decay of dipolar order T_1^d was found to depend strongly on the impurity type and concentration. Furthermore, T_1^d could be either longer or shorter than the rotating-frame spin-lattice relaxation time T_1^r . Measurements of relaxation phenomena in the laboratory frame and the rotating frame on the same crystals used to study spin-lattice relaxation of dipolar order are reported to provide information for the development of a theory.

II. THEORY

In the presence of a large static magnetic field \vec{B}_0 , a nuclear spin system will come into thermal equilibrium at the lattice temperature T_L . In this state the spin system can be described by a density matrix of the form

$$\rho \propto \exp[-(H_Z + H_d')/kT_L], \quad (1)$$

where

$$H_Z = -\gamma\hbar B_0 \sum_m I_{Zm}$$

is the usual Zeeman interaction of the spins with \vec{B}_0 and H_d' is the secular part of the nuclear dipole-dipole interaction⁷ H_d . The nonsecular part of H_d is neglected due to its nonresonant character.⁸ Since $H_Z \gg H_d'$, most of the spin system's energy will reside in the observable magnetization associated with the net alignment of spins along \vec{B}_0 , which is termed Zeeman order. This Zeeman order may be transferred to dipolar order by the ADRF method mentioned above. Dipolar order is characterized by a net alignment of spins along their individual local dipolar fields, which is a state of zero magnetization because of the completely random orientations of the local fields. The spin-lattice relaxation of this ordered dipolar state is characterized by the time constant T_1^d associated with the exponential decay of dipolar order, which may be monitored by reversing the ADRF process.^{5,9}

Jeneer and Broekaert¹⁰ (hereafter JB) have proposed a pulse method for preparing the nuclear spin system in a state apparently equivalent to the ordered dipolar state achieved through ADRF. Although this method has only about one-half the efficiency of the ADRF method, it requires a simpler apparatus and allows observation of short T_1^d 's. These authors show that maximum transfer of Zeeman order to dipolar order occurs when a $\frac{1}{2}\pi$ pulse which is phase shifted by $\frac{1}{2}\pi$ radians

and which occurs at the point of maximum slope in the free-induction decay resulting from the first pulse.

Lowe and Tse² have solved the transport equation for the rotating-frame magnetization $M^r(t)$, and they have obtained expressions for the rotating-frame spin-lattice relaxation time T_1^r for three limiting cases:

rapid diffusion: $R > b^r \gg \beta^r$ ($1 \gg \delta^r > \Delta^r$)

$$(T_1^r)^{-1} \approx \frac{4}{3} \pi N_p \bar{C}^r (b^r)^{-3} \propto B_1^2; \quad (2)$$

diffusion limited: $R \gg \beta^r \gg b^r$ ($\delta^r \gg 1 \gg \Delta^r$)

$$(T_1^r)^{-1} \approx \frac{8}{3} \pi N_p (\bar{C}^r)^{1/4} (D^r)^{3/4} \propto B_1^{1/2}; \quad (3)$$

diffusion vanishing⁶: $R \approx \beta^r \gg b^r$ ($\delta^r \gg \Delta^r \gtrsim 1$)

$$(T_1^r)^{-1} \approx 37 (\bar{C}^r D^r)^{1/2} N_p^{4/3} \propto B_1; \quad (4)$$

where the given field dependencies are valid only for the condition of $\omega_1 \tau_c \gg 1$. N_p is the paramagnetic-impurity concentration, which in the first two cases is assumed low enough that only one impurity ion is important in determining the relaxation rate in a given region of radius R , where

$$R = \left(\frac{3}{4} \pi N_p\right)^{1/3}. \quad (5)$$

b^r is the rotating-frame diffusion barrier radius, D^r and \bar{C}^r are the coefficients of the spin diffusion and direct relaxation terms, respectively, in the rotating-frame magnetization transport equation, and $\beta^r = (\bar{C}^r/D^r)^{1/4}$. \bar{C}^r is an average over all angles and is given by

$$\bar{C}^r = \gamma_p^2 \gamma_n^2 \hbar^2 S(S+1) \left(\frac{4}{15} \frac{\tau_c}{1 + \omega_1^2 \tau_c^2} + \frac{1}{5} \frac{\tau_c}{1 + \omega_0^2 \tau_c^2} \right), \quad (6)$$

where γ_p and γ_n are the magnetogyric ratios of the impurity ions and nuclear spins, respectively. S is the impurity spin quantum number, τ_c is the

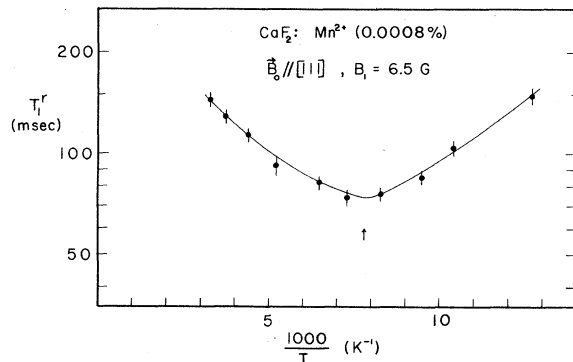


FIG. 1. $\text{Log}_{10} T_1^r$ vs $1000/T$ with the minimum indicated at about 128 K.

correlation time associated with the motion of the impurity spins,

$$\omega_1 = \gamma_n B_1, \quad \omega_0 = \gamma_n B_0, \quad \Delta^r = \frac{1}{2} (\beta^r/R)^2,$$

and

$$\delta^r = \frac{1}{2} (\beta^r/b^r)^2, \quad D^r = 6.5 \times 10^{-13} \text{ cm}^2/\text{sec},$$

using Kim's¹¹ value for the laboratory-frame diffusion coefficient D and $D^r = \frac{1}{2} D$.

As indicated in (2)–(4), the three diffusion cases may be distinguished by the way in which T_1^r depends upon the rf field B_1 . The diffusion-vanishing case is further unique in its nonlinear dependence of $(T_1^r)^{-1}$ on N_p . In addition, Tse and Lowe⁶ show that the initial decay of $M^r(t)$ for the diffusion-vanishing case (and to a much lesser extent for the diffusion-limited case) follows a $t^{1/2}$ law, where

$$M^r(t) = M^r(0) \left[1 - \frac{4}{3} \pi^{3/2} N_p (\bar{C}^r)^{1/2} t^{1/2} \right]. \quad (7)$$

Therefore, a graph of $[M^r(0) - M^r(t)]/M^r(0)$ vs $t^{1/2}$ will yield a straight line of slope

$$S^r = \frac{4}{3} \pi^{3/2} N_p (\bar{C}^r)^{1/2}. \quad (8)$$

This is a particularly useful relationship because a measurement of S^r can be used to determine N_p or τ_c , if the other has been previously determined. τ_c may be independently determined over a wide temperature range by locating the minimum in the T_1^r -vs- $1/T$ curve and applying Leushin's¹² theory for the temperature dependence of τ_c , which applies to S-state ions (such as Mn^{2+}) in diamagnetic crystals having the CaF_2 symmetry.

III. EXPERIMENT

The phase-coherent pulse NMR spectrometer used in this work was typical of those reported in the literature. The gated power amplifier was a modification of one designed by Lowe and Tarr.¹³ The rf field B_1 produced by this amplifier yielded $\frac{1}{2} \pi$ pulses of approximately 5- μsec duration and spin-locking pulses of up to 30-msec duration. The slowly decreasing ADRF pulse was produced

TABLE I. τ_c values for Mn^{2+} ions: obtained from a T_1^r minimum, Leushin's (Ref. 6) theory, and $t^{1/2}$ slopes S^r .

Temperature (K)	τ_c (sec)
298	4.8×10^{-7}
128	6.1×10^{-6}
77	4.7×10^{-5}
63	1.4×10^{-4}
4.2	1.1×10^{-3}

TABLE II. ^{19}F relaxation times for the Mn-1 sample with \vec{B}_0 parallel to the crystalline axis indicated.

T (K)	T_1 (sec)			T_1^d , ADRF (msec)		T_1^d , JB (msec)		T_1^r (msec) $B_1 \approx 10$ G [111]
	[111]	[110]	[100]	[111]	[100]	[111]	[100]	
298	6.8			280		285		124
80				238	242	208	203	
77	21	18	14			187		126
63				212		163		
4.2	127	123	92	782	720	788	716	>300

by external modulation of the master oscillator and had a duration of 8 msec. The field \vec{B}_0 was produced by a 12-in. electromagnet. Tests using the proton resonance in water had previously shown this magnet to have a static field inhomogeneity of less than 10 mG over the sample volume at a field strength of 5 kG.¹⁴ In this work the field strength was adjusted for a ^{19}F Larmor frequency of approximately 23 MHz.

T_1 measurements utilized the $\frac{1}{2}\pi - \tau - \frac{1}{2}\pi$ pulse technique, and the usual $\frac{1}{2}\pi$ -spinlock procedure³ was used in measuring T_1^r . Preparation of the ordered dipolar state was accomplished by both methods mentioned in Sec. II. The amount of dipolar order remaining at any time t after preparation of the state was monitored by a $\frac{1}{4}\pi$ information pulse, which eliminates the need for converting dipolar order back into Zeeman order by producing a dipolar signal directly.^{9,15} In making the T_1^d measurements, care was taken to insure that the reference signal to the phase-sensitive detector was in quadrature with the Zeeman signal.

The three single crystals of CaF_2 used in these experiments were obtained from Optovac, Inc. (North Brookfield, Mass. 01535). Each was cylindrically shaped ($\frac{3}{8}$ in. diam by $\frac{1}{2}$ in. long) with the cylindrical axis parallel to the [110] crystalline axis. Ion concentrations supplied by Optovac for the three crystals were 0.001% Mn^{2+} (Mn-1), 0.1% Mn^{2+} (Mn-2), and 0.05% Ce^{3+} by weight. As described in Sec. IV, the effective ion concentrations of the Mn^{2+} samples were experimentally de-

TABLE III. ^{19}F relaxation times for the Mn-2 sample with \vec{B}_0 parallel to the [111] crystalline axis.

T (K)	T_1 (sec)	T_1^d (msec)	T_1^r (msec) $B_1 \approx 9$ G
298	0.4	<10, ADRF	2.5
77	1.1	5.6, JB	2.0
4.2	3.5	<10, ADRF	8.0

termined. Neutron activation analysis has shown the Ce^{3+} concentration to be 0.074% by weight.

IV. RESULTS AND DISCUSSION

A. Determination of N_p and τ_c for Mn^{2+} samples

T_1^r was measured as a function of temperature for the Mn-1 sample. Only one T_1^r minimum was observed in the temperature range 298–4.2 K, indicating the presence of only one impurity. Figure 1 shows this minimum to occur at about 128 K

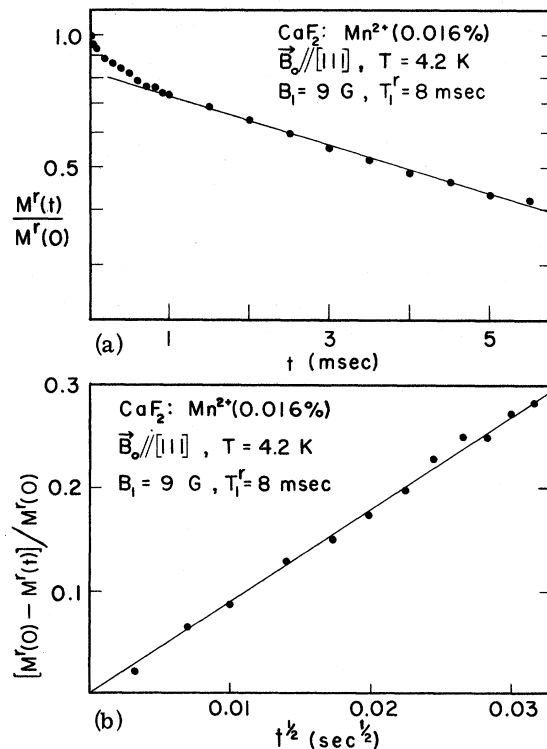


FIG. 2. (a) $\log_{10} [M^r(t)/M^r(0)]$ vs t showing a non-exponential decay of the initial magnetization; (b) $[M^r(0) - M^r(t)]/M^r(0)$ vs $t^{1/2}$ using the initial non-exponential points of (a).

TABLE IV. $t^{1/2}$ slopes S^r from T_1^r curves and calculations of parameters Δ^r and δ^r for the Mn-1 sample with $B_1 > B_{loc}$ and $T = 77$ K.

B_1 (G)	S^r (sec $^{-1/2}$)	N_p (apparent)	Δ^r	$\frac{1}{2}(\beta^r/b)^2$	δ^r
10.1	1.5	4.92×10^{17}	0.41	8.33	$\gg 1$
6.4	2.1	4.43×10^{17}	0.60	13.09	$\gg 1$
4.8	2.6	4.14×10^{17}	0.76	17.34	$\gg 1$
2.8	3.5	3.34×10^{17}	1.04	28.90	$\gg 1$
1.5	4.8	2.70×10^{17}	1.61	49.10	$\gg 1$

with $B_1 = 6.5$ G. This agrees quite well with the $\text{CaF}_2:\text{Mn}^{2+}$ data of Tse and Lowe.⁶ The condition for a T_1^r minimum, $\omega_1\tau_c = 1$, was used to find τ_c at 128 K. Leushin's¹² theory giving the temperature dependence for electron-spin-lattice relaxation was then used to calculate τ_c at 77 and 63 K. These values for τ_c are given in Table I.

The relaxation times T_1 and T_1^r as measured for the Mn-1 and Mn-2 samples are summarized in Tables II and III, respectively. The notation > 300 msec indicates that T_1^r was longer than the spectrometer was capable of measuring. T_1^r curves for the Mn-2 sample exhibited an initial nonexponential dependence at 198, 77, and 4.2 K. An example of this nonexponential decay is shown in Fig. 2(a). It has been pointed out that inhomogeneous doping can cause an initial nonexponential decay¹⁶; however, this type of nonexponential dependence should occur in both the laboratory and rotating frames and at all temperatures and values of B_1 . The Mn-1 sample only exhibited a nonexponential dependence at 77 K in the rotating frame, and no deviation from the exponential was observed in the laboratory frame for either Mn^{2+} sample. Also, the nonexponential decays reported here were strongly dependent upon the value of B_1 . Therefore, these nonexponential decays are the result of the $t^{1/2}$ law associated with the diffusion-

vanishing or diffusion-limited conditions and are not due to inhomogeneous doping. A plot of $[M^r(0) - M^r(t)]/M^r(0)$ vs $t^{1/2}$ for the initial points of Fig. 2(a) is shown in Fig. 2(b). The points are indeed linear with an approximate slope of $8.9 \text{ sec}^{-1/2}$. The slopes S^r for several $[M^r(0) - M^r(t)]/M^r(0)$ -vs- $t^{1/2}$ curves and the corresponding parameters Δ^r and δ^r are given in Tables IV and V, where calculations at 298 and 4.2 K assumed $\tau_c \approx 10^{-6}$ sec and $\tau_c \approx 10^{-3}$ sec, respectively. These choices for τ_c were based on an intuitive extrapolation of Leushin's theory. For fields on the order of a kilogauss and at room temperature or less, $\omega_0\tau_c \gg 1$ for Mn^{2+} ions such that $b^r \ll b$ and

$$\delta^r \gg (\beta^r/b)^2, \quad (9)$$

where b is the diffusion-barrier radius in the laboratory frame.² In addition, $S = \frac{5}{2}$ and $\gamma_p^2 \hbar^2 S(S+1) = 3 \times 10^{-39} \text{ (erg/G)}^2$ for Mn^{2+} ions.⁶

Consistent values for the effective N_p using (8) were obtained only when the diffusion-vanishing condition $\Delta^r \geq 1$ occurred with B_1 greater than the local field. Such experimental values for the effective N_p of the Mn^{2+} samples are given in Table VI. These values were calculated using the S^r data with $\Delta^r > 1$ at 77 K where τ_c was known from Leushin's theory using the value of τ_c calculated at the minimum shown in Fig. 1. With N_p known, τ_c was calculated at 298 and 4.2 K by again using (8) and the S^r 's for the Mn-2 sample corresponding to the largest Δ^r in Table V. These values for τ_c are shown in Table I, and they agree quite well with the extrapolations given above.

The experimental values for N_p given in Table VI may be independently checked by making a log-log plot of T_1 and T_1^r vs N_p and comparing the slopes obtained with the expected exponent dependence of T_1 and T_1^r on N_p . These two plots are shown in Fig. 3, where $B_1 \approx 9.5$ G. Since a large portion of the $\bar{M}^r(t)$ decay curves for these two Mn^{2+} samples obeyed the $t^{1/2}$ law at 77 K and since T_1^r for the Mn-1 sample was found to be pro-

TABLE V. $t^{1/2}$ slopes S^r from T_1^r curves and calculations of parameters Δ^r and δ^r for the Mn-2 sample with $B_1 > B_{loc}$.

T (K)	B_1 (G)	S^r (sec $^{-1/2}$)	N_p (apparent)	Δ^r	$\frac{1}{2}(\beta^r/b)^2$	δ^r
R.T.	9.0	20.6	3.99×10^{18}	2.82	37.65	$\gg 1$
77	9.0	18.7	5.52×10^{18}	2.30	9.33	$\gg 1$
4.2	9.0	8.9	12.06×10^{18}	0.84	1.26	$\gg 1$
4.2	6.2	9.6	8.96×10^{18}	0.99	1.83	$\gg 1$
4.2	3.6	11.6	6.29×10^{18}	1.36	3.15	$\gg 1$
4.2	1.7	20.8	5.33×10^{18}	2.59	6.66	$\gg 1$

TABLE VI. Mn^{2+} ion concentration data.

Sample	N_p , by manufacturer (10^{18} ions/cm 3)	N_p , by measurement (10^{18} ions/cm 3)	(% by wt.)	R (10^{-8} cm)
Mn-1	0.348	0.28	0.0008	94.8
Mn-2	34.8	5.6	0.016	34.9

portional to the first power of B_1 at 77 K as shown in Fig. 4, T_1^r was expected to be inversely proportional to the $\frac{4}{3}$ power of N_p , corresponding to the diffusion-vanishing case. The slope of -1.4 obtained for $\log_{10} T_1^r$ vs $\log_{10} N_p$ differs from the expected result by 5%. Since these samples were not diffusion vanishing in the laboratory frame, the slope of -1.0 obtained for $\log_{10} T_1$ vs $\log_{10} N_p$ is exactly what was expected.

B. Spin-lattice relaxation of dipolar order

The ordered dipolar state and the methods used to prepare and detect its order have been discussed above. T_1^d measurements for the three samples are given in Tables II, III, and VII. The notation <10 msec indicates that T_1^d was shorter than could be measured by the ADRF method. The

T_1^d 's obtained at 77 K using the JB preparation method indicate T_1^d to be inversely proportional to the 1.2 power of the Mn^{2+} ion concentration. Figure 5 shows a graph of $\log_{10} T_1^d$ vs $1000/T$ for both the ADRF and JB T_1^d 's. Although the two methods yielded essentially identical T_1^d 's at 298 and 4.2 K, the JB T_1^d was 24% lower than its ADRF counterpart at 63 K and 15% lower at 80 K. No orientational dependence was indicated at 80 K, but both preparation methods had equal orientational dependence at 4.2 K.

Using both dipolar-state preparation methods, a large portion of the initial decay of dipolar order in the Mn-1 sample at 4.2 K was nonexponential. However, as shown in Fig. 6, approximately 30% of the dipolar order was lost in this region with the ADRF method compared to about 15% for the JB method. This sample also exhibited an initial nonexponential decay at 80 K, but no deviation from exponential was observed at 298 K. The

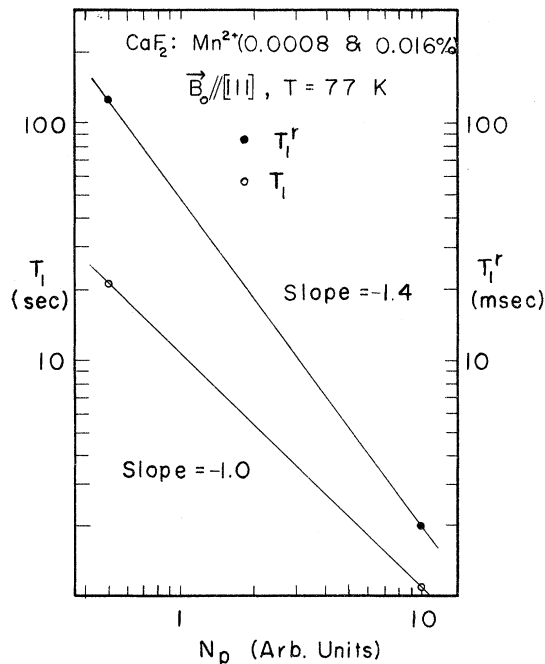


FIG. 3. $\log_{10} T_1$ and $\log_{10} T_1^r$ vs $\log_{10} N_p$, where the experimental N_p 's were used and the T_1^r measurements were made with $B_1 \approx 9.5$ G.

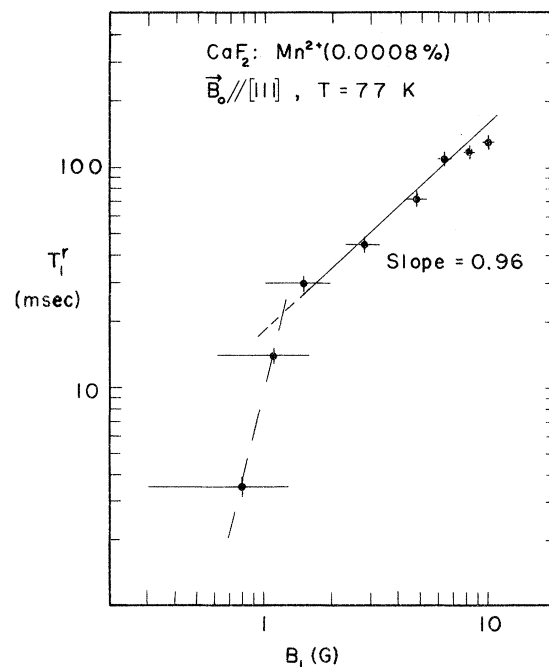


FIG. 4. $\log_{10} T_1^r$ vs $\log B_1$ with the Mn-1 sample.

TABLE VII. ^{19}F relaxation times in $\text{CaF}_2:\text{Ce}^{3+}$ (0.074 wt%) with B_0 parallel to the [111] crystalline axis.

Temperature (K)	T_1 (msec)	T_1^d , ADRF (msec)	T_1^r (msec) $B_1 \approx 10$ G
298	600	124	>300
4.2	780	<10	9.7

Mn-2 sample, with its higher concentration of Mn^{2+} ions, exhibited a much more enhanced initial nonexponential decay. By analogy to the rotating-frame case, the nonexponential portion of each T_1^d curve was graphed as $[M^d(0) - M^d(t)]/M^d(0)$ vs $t^{1/2}$. The curves were approximately linear with slopes S^d as given in Table VIII. A comparison of S^d and S^r for the Mn^{2+} samples at nitrogen temperatures indicates that both slopes have the same dependence on the impurity concentration.

Since ADRF includes the spin-locked state of the rotating-frame magnetization as an intermediate step, one might expect T_1^d to correspond in some way to T_1^r for sufficiently small values of B_1 . For example, Fig. 5 indicates a minimum in the $\log_{10} T_1^d$ -vs- $1000/T$ curve which, in comparison with Fig. 1, is significantly shifted in the direction expected for a T_1^r minimum with a low B_1 value.⁶ However, the slopes S^d were much less than the slopes S^r which increased with decreasing B_1 . Figure 4 shows $\log_{10} T_1^r$ as a function of $\log_{10} B_1$ for the Mn-1 sample at 77 K, and a similar curve was obtained for the Mn-2 sample at 4.2 K. A change in the basic rotating-frame relaxation process is indicated at $B_1 \approx B_{1oc}$, where T_1^r rapidly approaches times the order of T_2 for lower values of B_1 . Clearly, T_1^d is not the limit of T_1^r as B_1 goes to zero. In fact, T_1^d was observed to be

greater than T_1^r in the Mn^{2+} samples even with $B_1 \approx 10$ G. In contrast, T_1^d was never observed to be greater than T_1^r in the Ce^{3+} sample.

V. CONCLUSION

The results of these experiments indicate that an accurate determination of the effective impurity concentration N_p using experimental $t^{1/2}$ slopes is only possible when $\delta^r \gg \Delta^r \approx 1$, which is the Lowe-Tse diffusion-vanishing condition in the rotating frame.

T_1^d has been found to be inversely proportional to the 1.2 power of N_p in $\text{CaF}_2:\text{Mn}^{2+}$ samples. An orientational dependence for T_1^d was observed at 4.2, but not at 80 K, whereas T_1 was orientation-

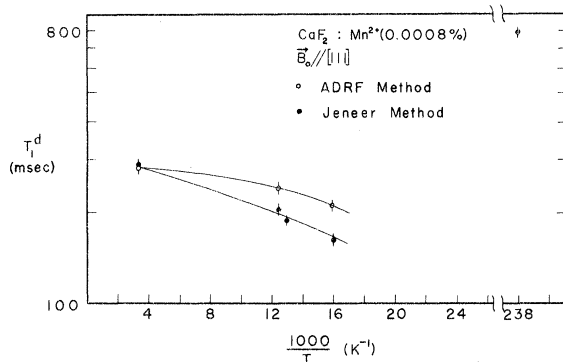


FIG. 5. $\log_{10} T_1^d$ vs $1000/T$ from 298 to 4.2 K, where both the ADRF (upper curve) and JB (lower curve) preparation methods were used.

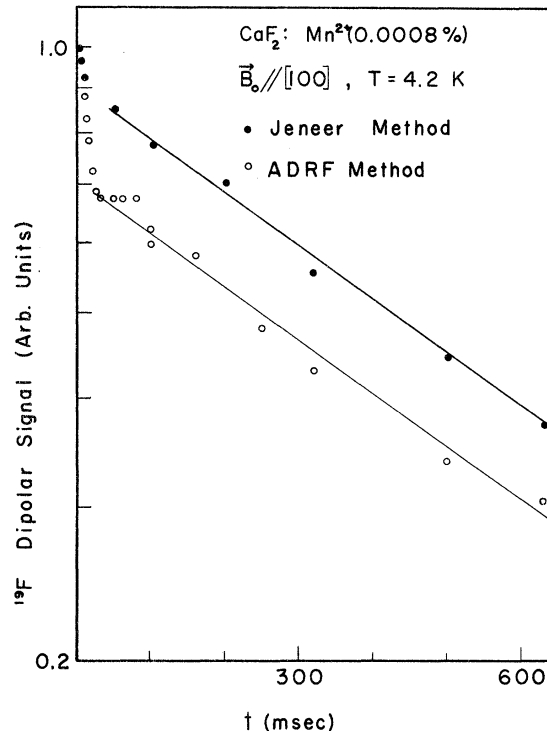


FIG. 6. $\log_{10}^{19}\text{F}$ dipolar signal vs t for both the ADRF (lower curve) and JB (upper curve) preparation methods.

TABLE VIII. $t^{1/2}$ slopes S^d from T_1^d curves of the Mn^{2+} samples with B_0 parallel to [111] at 80 and 77 K and B_0 parallel to [100] at 4.2 K.

T (K)	Mn-1: S^d (sec $^{-1/2}$)		Mn-2: S^d (sec $^{-1/2}$)
	ADRF	JB	
80	2.1	1.1	
77			14.0
4.2	2.0	1.1	

ally dependent at both 4.2 and 77 K. Although the dipolar signals obtained from both the ADRF and JB preparation methods are quite similar, there

are differences in the resulting dipolar relaxation which are greater than can be attributed to experimental error. For example, the JB T_1^d 's were 24 and 15% lower than the corresponding ADRF T_1^d 's at 63 and 80 K, respectively. In addition, the loss in dipolar signal due to $t^{1/2}$ decay was twice as great for the ADRF method. Therefore, there appears to be a basic difference in the states achieved by these two dipolar-state preparation methods.

No correlation between T_1^d and T_1^r was observed. T_1^d was less than T_1^r in the $CaF_2:Ce^{3+}$ sample, but it was greater than T_1^r in the $CaF_2:Mn^{2+}$ samples. A T_1^d minimum was observed between 63 and 4.2 K for the Mn-1 sample, but no such minimum was observed for the Ce^{3+} sample.

†Work supported in part by the National Science Foundation under Grant No. NSF-GP-23293.

*Physics Dept. (TRMP), M. D. Anderson Hospital and Tumor Institute, Houston, Tex. 77025.

¹N. Bloembergen, *Physica (Utr.)* **15**, 386 (1949).

²I. J. Lowe and D. Tse, *Phys. Rev.* **166**, 279 (1968).

³S. R. Hartmann and E. L. Hahn, *Phys. Rev.* **128**, 2042 (1962).

⁴D. A. McArthur, E. L. Hahn, and R. E. Walstedt, *Phys. Rev.* **188**, 609 (1969).

⁵F. M. Lurie and C. P. Slichter, *Phys. Rev.* **133**, A1108 (1964).

⁶D. Tse and I. J. Lowe, *Phys. Rev.* **166**, 292 (1968).

⁷J. H. Van Vleck, *Phys. Rev.* **74**, 1168 (1948).

⁸C. P. Slichter and W. C. Holton, *Phys. Rev.* **122**, 1701 (1961).

⁹A. G. Anderson and S. R. Hartmann, *Phys. Rev.* **128**,

2023 (1962).

¹⁰J. Jeneer and P. Broekaert, *Phys. Rev.* **157**, 232 (1967).

¹¹K. H. Kim, Ph.D. thesis (University of Pittsburgh, Pittsburgh, 1969) (unpublished).

¹²A. M. Leushin, *Fiz. Tverd. Tela* **5**, 851 (1963) [*Sov. Phys.-Solid State* **5**, 623 (1963)].

¹³I. J. Lowe and C. E. Tarr, *J. Sci. Instrum.* **1**, 604 (1968).

¹⁴D. K. Hutchins and S. M. Day, *Phys. Rev.* **180**, 432 (1969).

¹⁵J. Jeneer, *Advances in Magnetic Resonance*, edited by J. S. Waugh (Academic, New York, 1968), Vol. 3, pp. 205-310.

¹⁶D. C. W. Tse, Ph. D. thesis (University of Pittsburgh, Pittsburgh, 1965) (unpublished).